Aerodynamic Performance of Smooth Selectively Superhydrophobic Flat Plates: A Numerical Approach

VC Perera[1#] and SLMD Rangajeewa[1]
[1] *Faculty of Engineering, General Sir John Kotelawala Defence University, Ratmalana, Sri Lanka*
[#]37-eng-0054@kdu.ac.lk

Abstract *- The interference to fluid flow over a solid surface is significantly high to such an extent that the fluid in contact with the surface possesses a null velocity. This phenomenon is called the no-slip condition. On the contrary, superhydrophobic surfaces possess significant slip velocities, hence a partial slip condition, enabling significant drag reduction properties when in relative motion with fluids. However, making a complete object superhydrophobic may not necessarily provide the most aerodynamic nor cost-effective solution. A smooth flat plate of 50% slip condition was used as the first step to link the relationship between superhydrophobic area and the drag coefficient using computational fluid dynamics software, OpenFOAM. A greater drag reduction was observed for partially superhydrophobic flat plates compared to a fully superhydrophobic counterpart. The flat plate was made superhydrophobic using five unique approaches in total, both unilaterally and bilaterally in either direction of the flat plate. It was then found that drag reduction did not arbitrarily depend on the total area of superhydrophobicity. Each approach resulted in a unique drag reduction trend with increasing superhydrophobic area. Superhydrophobising the flat plate from the trailing edge towards the leading edge, against the flow direction, provided the best drag reduction characteristics.*

Keywords **- Superhydrophobic, Flat Plate, Drag Reduction.**

I. INTRODUCTION

The study of Aeronautics continues to push the boundaries of effective and efficient aircraft design over time. One such notable attempt in the past decade is NASA's Environmentally Responsible Aviation (ERA) project (Merlin, 2020), initiated primarily to reduce fuel burn, nitrous oxide (NOx) emissions and community noise footprints. However, enhancing the aerodynamics of airfoils, hence their drag reduction capabilities, to reduce fuel burn without employing retrofit devices are a feat of engineering yet to be achieved. Macro-scaled technologies are the most commonly sought-after mode of achieving such goals: changing airfoil geometries, performance enhancement devices and active or passive flow control methods. Despite complex, macro-scaled technologies drawing the most attention, nano-scaled technologies have proven to make greater advancements in a variety of fields.

One such breakthrough in nanotechnology is the discovery of superhydrophobic surfaces. Despite being highly reviewed in a variety of industries, their feasibility in aerospace applications have rarely been evaluated. Potential applications for the use of superhydrophobic surfaces in the aerospace industry owe to their lucrative properties of corrosion resistance (Ma et al., 2018), (Xu et al., 2019), (Zhang et al., 2015), Anti-icing (Latthe et al., 2019), Anti-fouling (Sampathkumar et al., 2021), Self-cleaning (Rasitha et al., 2019), (Khan et al., 2021), and Drag reduction (Tanvir & Kietzig, 2016), (Barbier, Jenner & D'Urso, 2014), (Ou, Perot & Rothstein, 2004).

At an engineering perspective: how exactly does superhydrophobic surfaces perform with regards to aerodynamics? Using known properties of the surfaces, it is possible to test them in a virtual setup using Computational Fluid Dynamics (CFD) software. This helps in informed decision making in aerodynamic design, well before the technology is available for the market, saving both time and resources. Simulations have yielded that a fully superhydrophobic airfoil accounts for a 66% increase in the lift coefficient (C_L) and 45% decrease in the drag coefficient (C_D) compared to a conventional airfoil (S.F. Chini, Mahmoodi & Mehran, 2017). This finding has been graphically represented in Figure 1. Consider a comparison between a partially superhydrophobic airfoil with one that is fully superhydrophobic, as depicted in Figure 2. Which airfoil would produce better aerodynamic properties? Developing a solid relationship between superhydrophobic area, (as a function of the chord length) and the respective aerodynamic parameters, C_D and C_L, as depicted in Figure 1 will help answer this question. By connecting the dots, the research gap in the aerodynamic performance of partially superhydrophobic airfoils can be closed. Thus, the objective of this research is to simulate flow past a selectively superhydrophobic flat plate, as a first step, to determine what degree of superhydrophobising is the most efficient, aerodynamically, and economically: fully or partially?

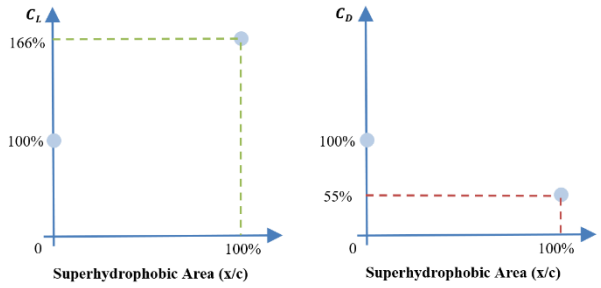

Figure 1 - Research gap.

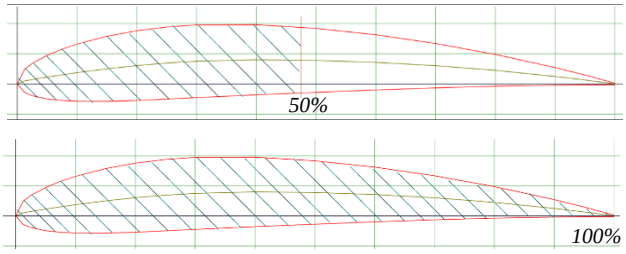

Figure 2 - 50% superhydrophobic vs fully superhydrophobic.

II. METHODOLOGY & EXPERIMENTAL DESIGN

The novel concept was tested out using the OpenFOAM software on a flat plate, by measuring the resulting coefficient of drag (C_D) for the area of the flat plate made superhydrophobic. The fluid flow parameters were set such that a laminar airflow was introduced, similar to the study conducted by Chini et al. However, the present study took into consideration a fixed angle of attack of the object, at $\alpha = 0°$.

There are two conditions by which an object is characterized as a superhydrophobic surface. The first is its characteristic surface roughness in the nanoscale (Wenzel, 1936), (Cassie & Baxter, 1944). Water droplets reside and slide over the characteristic nanostructures present on the surface as shown in Figure 4 b). The second characteristic is that superhydrophobic surfaces possess a partial slip-condition at the surface, which usually takes a value of up to 60% of that of the freestream velocity (Ou, Perot & Rothstein, 2004) as a virtue of its low surface free energy (SFE). The partial slip condition was set to 50% in this study to match the maximum partial slip condition utilized by Chini et al.

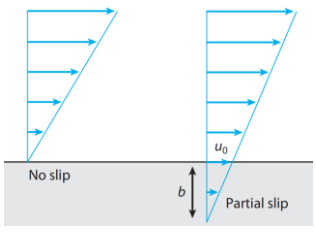

Figure 3 - Partial Slip Condition
Source: (Rothstein, 2010)

This study assumes that the surface is a perfectly smooth surface as initially assumed at the early stages of developing superhydrophobic surfaces, expressed through the Young's Equation (Young, 1805). The inability to consider a nanoscaled roughness on the solid model of the flat plate restricts the true drag reduction capabilities of the superhydrophobic surface. The uniform roughness of these surfaces play hosts to nanoscopic air pockets which allow for shear-free flow of fluids over them (Lee, Choi, & Kim, 2008). The trapped air between the nanoscopic troughs have a lubricating effect (Thurston & Jones, 1965), which gives these surfaces a natural degree of slip, characterized by the slip length, b, depicted in Figure 3. The slip length is defined as the distance between the top wall position and the depth at which the extrapolated velocity profile reaches zero velocity. Ordinary surfaces have a slip length less than 1 nm, while superhydrophobic surfaces have a slip length as large as 400 µm (Lee and Kim, 2009).

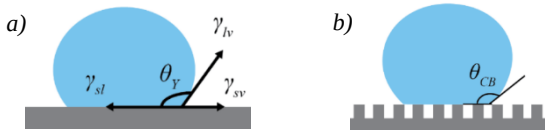

Figure 4 - a) Young's Equation; b) Cassie-Baxter State Source: (Tam, J. et al., 2016)

Only the second characteristic of superhydrophobic surfaces, that being the partial slip condition, is considered here. The flat plate will consist of boundary lines which divides it into three segments. User input into the block mesh directory allows the position of the boundary lines to vary as desired, such that the flat plate is segmented into desired percentage areas along the chord length. Figure 5 shows the segmented flat plate designed in its virtual environment for two cases in which the boundary line positioning was shifted to obtain the desired areas of segmentation (demarcated by different colors). The segments that are required to be superhydrophobic will be given a partial slip condition of 50%, while the remaining segments possess a no-slip condition so that it mimics the characteristics of a real surface. All segments will be given the no-slip condition or partial slip condition provided that a real flat plate or fully superhydrophobic flat plate is to be simulated, respectively.

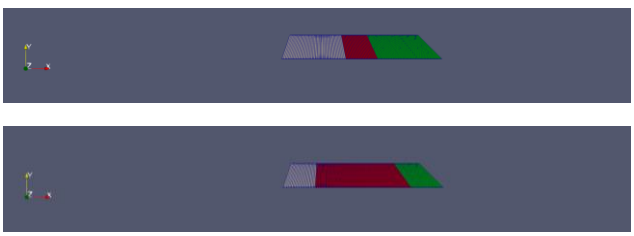

Figure 5 - Flat plate with variable segmentation areas.

Distinct blocks were then allocated over the segmented areas of the flat plate and ahead of its leading edge. Each block was characterized such that they would possess distinct meshing characteristics. The inlet section captures the flow entrance, followed by three other distinct blocks along the longitudinal axis to capture the flow over the three distinct surfaces of the flat plate. As the segmentation of the flat plate varied on a case-by-case basis, as previously depicted in Figure 5, so did the dimensions of each block. The consequence of this is represented in Figure 6. When the meshing constraints were left constant for all cases, the final mesh would also vary on a case by case basis. The final result for the coefficient of drag in such a scenario, would not purely be due to a change in superhydrophobic area, but could also result due to the changes in the mesh density across each block.

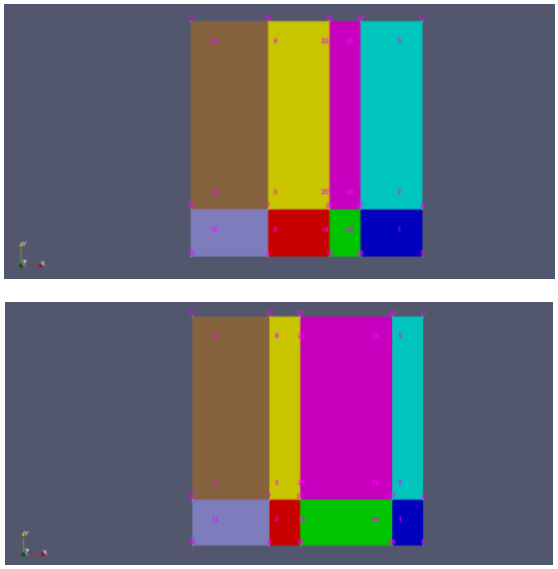

Figure 6 - Variation of block dimensions with each case.

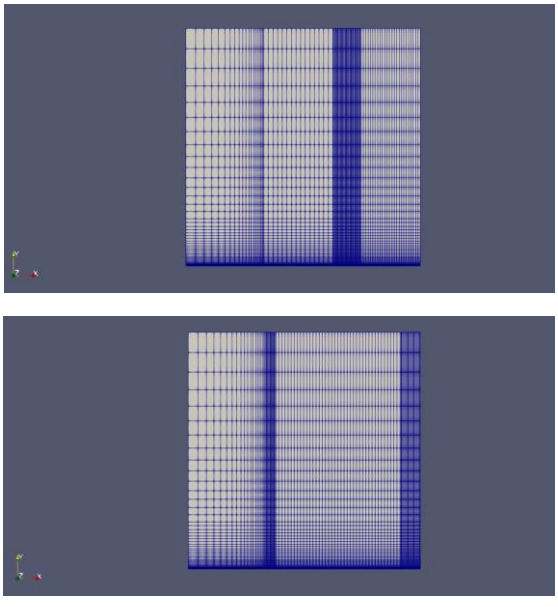

Figure 7 - Variation of mesh density with each case.

In order to ensure that the dependent variable, C_D, is measured solely due to the change in the independent variable only (superhydrophobic area), all other parameters are to be kept constant. Therefore, to achieve this the meshing constraints were systematically altered on a case-by-case basis, such that the final mesh for all cases remained virtually constant. Hence, the finalized mesh for all cases, regardless of the varying flat plate segmentation, is represented through Figure 8. The height of the cells were made to increase with the height at which they were located from the surface of the flat plate. This was to cater to the alternating requirements of the boundary layer region (bottom row of blocks) and the far field region (top layer of blocks) depicted in Figure 6. Despite being thin, the boundary layer region was given a considerable height and finer meshing so as to achieve greater clarity.

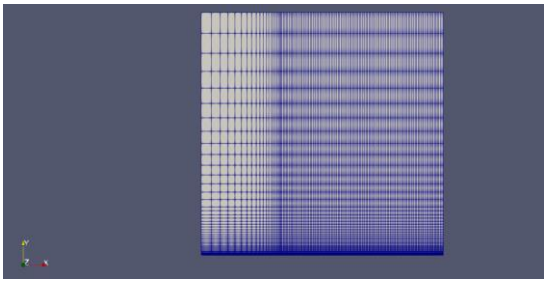

Figure 8 - Finalized mesh independent for all cases.

The spatial coordinates of the base of the flat plate's leading edge were set at x = 0. The flat plate extends to the edge of the mesh, longitudinally, as the study considers the case of an infinitely long flat plate. The meshing in the x-y plane, shown in Figure 8, has been extruded in the z-direction as the two dimensional flow over the flat plate is being considered. Table 1 below summarizes the boundary conditions utilized for the purpose of the simulation. Being an inherently transient solver, the icoFoam solver was made to utilize the initial conditions and boundary conditions for the case. The solver solves for incompressible, laminar Navier-Stokes equations using the Pressure-Implicit with Splitting of Operators (PISO) algorithm.

Table 1 - Boundary Conditions

Boundary Field	Type (Pressure)	Type (Velocity)
inlet	zeroGradient	fixedValue (internalField)
outlet	fixedValue (internalField)	zeroGradient
plate1	zeroGradient	partialSlip / noSlip
plate2		
plate3		
top	zeroGradient	fixedValue (internalField)
frontAndBack	empty	empty
symmBound	zeroGradient	zeroGradient

III. RESULTS

A. *Validation of Results*

The first step of the study was to simulate the flow over a real flat plate and compare the resulting C_D with the analytical solution. For a flat plate, the skin friction drag coefficient is a function purely based on the Reynolds number. The flow utilized in this study falls within the range $\mathrm{Re} < 500{,}000$. Hence it is considered laminar in nature (Ngo & Gramoll, 2010). Therefore, the coefficient of skin friction acting on a flat plate subjected to laminar flow across it is calculated using the dedicated expression:

$$C_{D,f} = \frac{1.328}{\sqrt{\mathrm{Re}}} = \frac{1.328}{\sqrt{5000}} = 0.01878$$

The value for C_D recorded by the OpenFOAM software for the real flat plate was, however, $C_D = 0.01968$. Thus, a deviation of +4.79% is recorded between the numerical value provided by the OpenFOAM software, and the analytical value calculated. This increase in the drag coefficient recorded by the numerical approach was considered to be fair, owing to the fact that the analytical equation above calculates the length averaged drag coefficient due to skin friction only.

Aerodynamic forces acting on a body are known to be a result of both shear stresses (caused by skin friction) and the pressure distribution acting over the body (Anderson, 2017). Although skin friction drag dominates flow parallel to a flat plate, it does not necessarily mean that the profile drag (which is the drag due to pressure) is zero for the same instance. It is assumed that the deviation in the values for the coefficient of skin friction drag is due to the ability of the OpenFOAM software to consider the profile drag simultaneously. Since the OpenFOAM software takes both sources of drag into consideration for calculating C_D, the resulting value for C_D can be deemed acceptable. The increase of 4.79% is then the contribution of profile drag to the total drag. Hence, the result for the numerical simulation is validated with reasoning.

The noSlip boundary condition for all three segments of the flat plate was switched to a partialSlip condition of valueFraction 0.5 to simulate the flow over a fully superhydrophobic flat plate. Figure 9 and Figure 10 show the velocity profile of the airflow over the real flat plate and fully superhydrophobic flat plate, respectively. Note how the partialSlip condition has increased the lower limit of speed from 0 m/s to 0.5 m/s in the case of a fully superhydrophobic flat plate. Figure 11 and Figure 12 show the respective pressure distributions over the flat plate. Both upper and lower limits of pressure for the flow over the flat plate have been subjected to change.

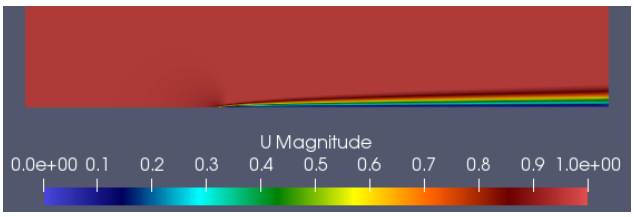

Figure 9 - Velocity profile (real plate).

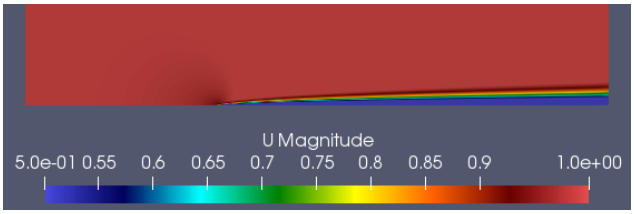

Figure 10 - Velocity profile (superhydrophobic plate).

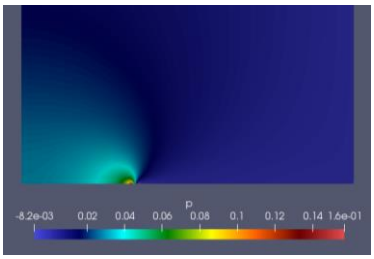

Figure 11 - Pressure distribution (real plate).

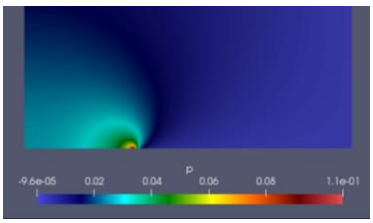

Figure 12 - Pressure distribution (superhydrophobic plate).

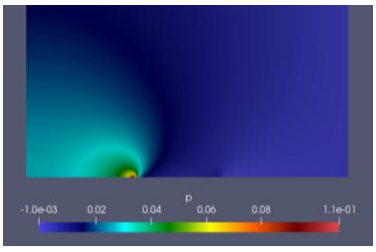

Figure 13 - Pressure distribution (40% superhydrophobic plate).

Boundary lines of the flat plate were then adjusted through the blockMeshDict to facilitate simulations for partial superhydrophobic conditions at regular 5% increments. The airflow was introduced for each case by running the simulation and the resulting C_D was recorded. Figure 13 shows the pressure distribution of a 40% partially superhydrophobic flat plate. Notice how the pressure distribution varies compared to a real flat plate and a superhydrophobic flat plate shown in Figure 11 and Figure 12, respectively. Additionally, a distinct reduction in

pressure manifests at the 40% mark of the flat plate in, as seen in Figure 13.

B. Superhydrophobising using a Singular Approach

The flat plate was made increasingly superhydrophobic, for 5% increments, starting from the leading edge (LE), working its way towards the trailing edge (TE) in the direction of airflow over the flat plate. For each case the resulting C_D was calculated. Figure 11 shows the variation in C_D with increasing superhydrophobic area. However, the aforementioned approach is not the only way that a flat plate could be made increasingly superhydrophobic. This gives rise to the question as to whether the C_D of a flat plate is arbitrarily dependent upon the superhydrophobic area, or would another superhydrophobising approach, if utilized, provide a different drag reduction trend?

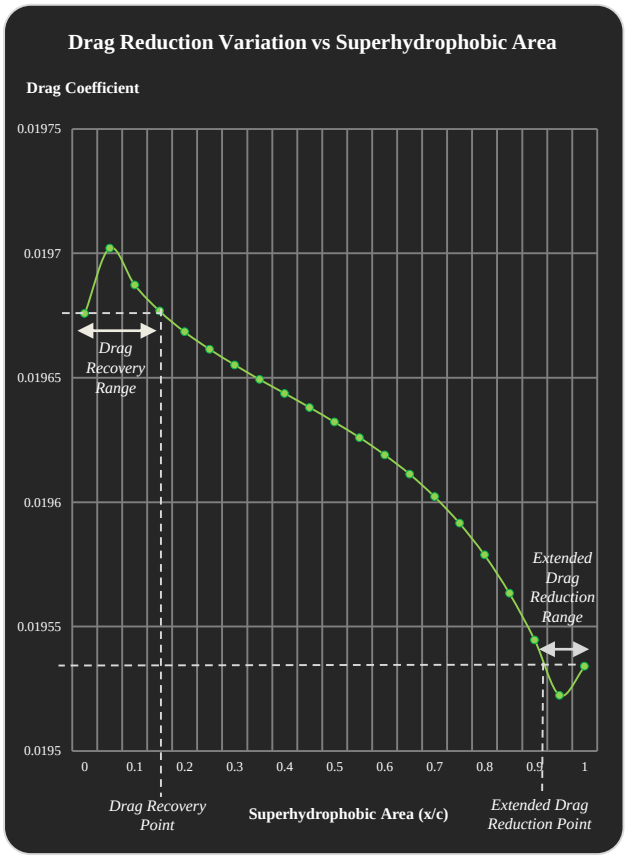

Figure 14 - Drag Reduction trend for Unilateral LE Approach.

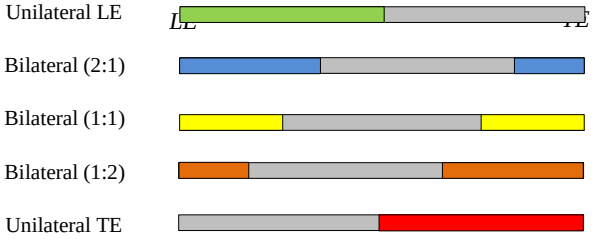

C. Superhydrophobising Using Multiple Approaches

Figure 15 - 50% superhydrophobicity by five unique approaches.

Take for example the case of the flat plate being made 50% superhydrophobic starting from the TE and working its way towards the LE, against the direction of airflow over the flat plate. If the superhydrophobic area was to increase from 0 – 100% in this direction, will the change in C_D still be the same as the initial approach? What if bilateral approaches of superhydrophobising were utilized? In order to answer these questions, five approaches by which the flat plate could be made selectively superhydrophobic at 5% increments, and were of potential importance to aerodynamic applications, were chosen as demonstrated in Figure 15. The drag reduction trends for each approach were plotted individually and then compared in Figure 16. The ratio in brackets for bilateral approaches represent the unit area by which the LE was made superhydrophobic to that by which the TE was made superhydrophobic.

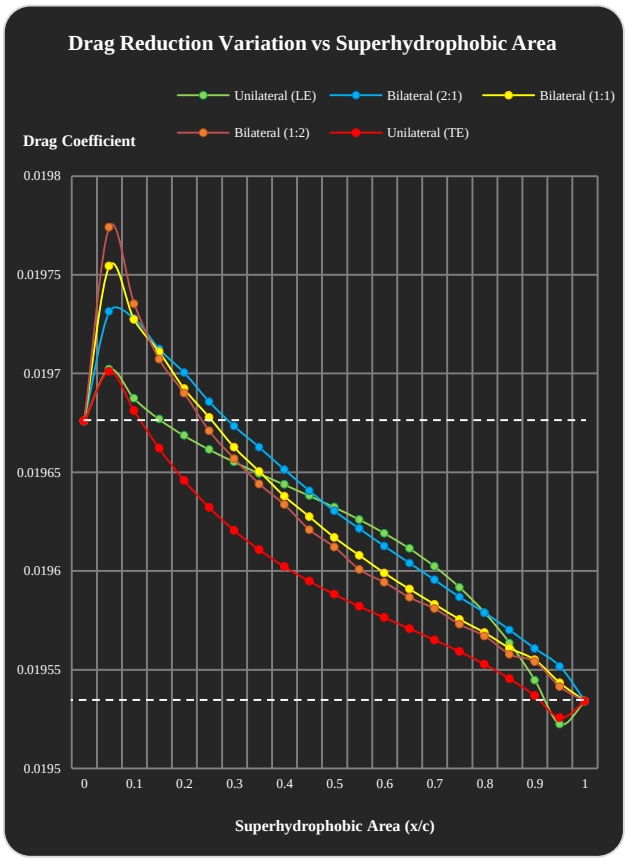

Figure 16 - Drag Reduction trend for Multiple Approaches.

IV. DISCUSSION

Flow over the flat plate originates from the LE and flows towards the TE. Hence, one would assume that providing the partial slip condition starting from the LE and moving towards the TE (Unilateral LE approach) would be the most suitable for achieving the best drag reduction capabilities. This will enable less resistance to the flow of the fluid as it first interacts with the LE before making its way towards the TE. However, the results of the experiment summarized in Figure 16 has completely disproven that the drag

reduction of a flat plate by providence of a partial slip condition is as trivial as assumed. The results have in fact proven that superhydrophobising the flat plate starting from the TE and moving towards the LE unilaterally (Unilateral TE approach), against the direction of flow of the fluid, provides better drag reduction characteristics. Comparing all five approaches together, the Unilateral TE approach consistently produced the lowest C_D in the $0-95\%$ superhydrophobic area range, making it the best approach overall.

For all five approaches, there is an initial drag increment as observed through the peaks of each trend in Figure 16. This is an undesirable outcome in an aeronautical perspective as aerodynamicists aim of achieving drag reduction instead of increasing drag. Since the partial slip condition allows for a reduction in the skin friction drag, the initial increase in the drag coefficient suggests an increase in total drag. This goes onto show the effect of how imposing the partial slip condition increases the profile drag over the flat plate to an extent which is much greater than the reduction in skin friction drag. The total drag of all five approaches reach a maximum at $5-6\%$ of superhydrophobic area, after which the total drag starts showing signs of reduction with increasing superhydrophobic area.

The superhydrophobic area of a partially coated flat plate which has a C_D equivalent to a real flat plate was termed the "drag recovery point", represented in Figure 14. Up until this point, there is no evidence of drag reduction capabilities by the partially superhydrophobic flat plate. In other words, the increase in the pressure drag was greater than the decrease in the skin friction drag up until this point, hence resulting in an overall increase in drag from the real flat plate configuration.

Through the observation of the five unique drag reduction trends produced by each approach, it is evident that the drag recovery point is dependent upon the approach utilized. The Unilateral TE approach showed the smallest drag recovery value, followed by the Unilateral LE approach. All three Bilateral approaches showed greater values for drag recovery compared to the Unilateral approaches, which is undesirable in an economic perspective. This means that a greater area of the flat plate had to be made superhydrophobic using these approaches in order to be able to achieve drag reduction, which thereby incur greater costs.

Note that the priority of superhydrophobising the TE in a Bilateral approach decreases with the following order: Bilateral (1:2), Bilateral (1:1) and Bilateral (2:1), as visualized using Figure 15. The Bilateral (1:1) approach provides equal priority in superhydrophobising both the trailing edge and leading edge, simultaneously. It is in the same order that the drag recovery points increase in value by roughly 2% with each approach, as observed in Figure 16. The Bilateral (1:2) approach is the first to reach a C_D value equivalent to that of the real flat plate amongst the three bilateral approaches, followed by Bilateral (1:1) and, finally, Bilateral (2:1) approach. This would mean, if a bilateral approach was to be utilized, prioritizing the superhydrophobising of the TE would produce better drag reduction characteristics, as made observable through Figure 16.

However, this is true only after a value of 12.5% superhydrophobic area along the chord length. At a value of 12.5% superhydrophobic area, the values of C_D for all three bilateral approaches converge to about 0.01972. For values of superhydrophobic area before 12.5%, prioritizing the superhydrophobising of the LE when utilizing bilateral approaches produced much less initial drag increments in comparison with a real flat plate. This is evident through the height of the initial peaks observed by each trend in relation to the datum drawn in Figure 16 through the C_D value of a real flat plate. For the case of the two unilateral approaches however, the opposite trend was observed, where the Unilateral TE approach produced a smaller drag increment compared to the Unilateral LE approach.

In terms of the stability of the approach utilized, once again, the Unilateral TE approach would surpass the Unilateral LE approach. This is because the Unilateral TE approach consistently provides better drag reduction characteristics in comparison with all the other approaches by being the first to reach the drag recovery point and maintaining a better drag reduction slope with increasing superhydrophobic area. The other approaches are subjected to a change in drag reduction performance with the range of superhydrophobic areas taken into consideration.

The Unilateral LE approach, despite seeming to be the most trivial approach for attaining drag reduction, is actually the most unpredictable. At the range of $0-30\%$ superhydrophobic area it would perform better than all bilateral approaches, while at a range of $30-50\%$ it would perform better than one or two other bilateral approaches. However, in the range of $50-80\%$ it would be the worst approach to consider for the partial superhydrophobising of a flat plate, from all of the five approaches.

Only at values exceeding 92.5% of superhydrophobic area will the Unilateral LE approach surpass the drag reduction capabilities of the Unilateral TE approach in being the best approach of partial superhydrophobising a semi-infinite flat plate.

Once again, it should be noted that further drag reduction capabilities are possible of being achieved had the nanoscopic roughness been integrated into the model

leading to the presence of shear free air-pockets. Despite the assumption of a smooth surface being utilized in this study, a drag reduction was still observed to such an extent that it surpassed a fully superhydrophobic plate in two out of five approaches, both of which are unilateral approaches.

Thus, this goes onto conclude that the partial superhydrophobising of a flat plate is confirmed to be more aerodynamically favorable than a fully superhydrophobic flat plate. The point at which the drag reduction surpasses that of a fully superhydrophobic flat plate was termed the "extended drag reduction point". Once again, the bilateral approaches were the least desirable, as they were unable to surpass a drag reduction beyond that of a fully superhydrophobic flat plate.

Therefore, for an engineer who has limited resources to use the superhydrophobic technology on a flat plate, partial superhydrophobising by means of a bilateral approach would not be the most aerodynamic nor cost-effective solution. Whether the goal is to follow a cost-effective approach or to achieving a coefficient of drag surpassing that of a fully superhydrophobic flat plate: the partial superhydrophobising of a flat plate by utilizing a unilateral approach would be the best.

With the data gathered, it can be concluded that the C_D of a partially superhydrophobic flat plate did not depend arbitrarily upon the superhydrophobic area but rather the approach utilized. The failure to deduce a relationship between the superhydrophobic area and aerodynamic parameters, leading to a failure in exploiting the optimal aerodynamic performance from the superhydrophobic technology has now been addressed for the case of a flat plate.

The formation of a superhydrophobic surface of uniform nanoscale roughness using nanosecond laser texturing can be extremely costly. A laser printing system costs $1,000,000 aside from the specialized metal powders it uses for printing, costing $400/kg (Shop3D.ca, 2020). Not knowing which degree of superhydrophobising produces optimal performance for an airfoil, or other objects of interest, leads to blind expenditures and a poor return on investment (ROI) – an unaffordable mistake in the Aerospace industry.

Through the results of this research, it is now clear that the research gap has been addressed for the case of an infinitely long flat plate, and the optimal superhydrophobising area is now clear for five different approaches of superhydrophobising utilized for the object.

V. FUTURE WORK

The present study focused on the drag reduction trend for an object of fixed geometry (infinitely long flat plate) for a fixed angle of attack and fixed Reynold's number. Aerodynamic characteristics of other partially superhydrophobic objects, such as cylinders and airfoils, for variable angles of attack and variable Reynolds numbers are other potential areas of interest to aerodynamicists in terms of research.

Having gained insights on the ability of partially superhydrophobic flat plates to perform better than a fully superhydrophobic flat plate, this newfound knowledge can then be translated to other objects of interest to aerodynamicists. A similar study if conducted on an airfoil will lead to much more significant findings in drag reduction and lift enhancement as airflow accelerates over an airfoil, unlike over a flat plate, due to its inherent camber.

The results of conducting a numerical study, similar to this, for the purpose of an airfoil, could then be compared with an experimental study. In such a case, all assumptions utilized by the numerical approach, especially the absence of a rough surface in the nanoscopic scale, will then be disregarded, leading to more reliable and practical solutions.

VI. CONCLUSION

In an attempt to relate the superhydrophobic area, as a function of the chord length of an object, with aerodynamic parameters, an infinitely long flat plate was utilized as a first step. It was found that a partially superhydrophobic flat plate performs better than a fully superhydrophobic flat plate and that the drag reduction capabilities were dependent upon the approach by which the flat plate was made superhydrophobic and not just the arbitrary value of the superhydrophobic area. For limited areas of superhydrophobicity in the range of up to 30%, whose exact ranges depended upon the approach taken, an increment in drag was also made evident.

REFERENCES

Anderson, J.D. (2017). Fundamentals of aerodynamics. New York, NY: McGraw Hill Education.

Barbier, C., Jenner, E. & D'Urso, B., 2014. Large Drag Reduction over Superhydrophobic Riblets. arXiv: *Fluid Dynamics* (physics.flu-dyn).

Cassie, A.B.D., and Baxter, S. (1944). Wettability of porous surfaces. *Transactions of the Faraday Society*, 40, p.546.

Chini, S.F., Mahmoodi, M. and Nosratollahi, M. (2017). The potential of using superhydrophobic surfaces on airfoils and hydrofoils: a numerical approach. 7(1), pp.44–44.

Khan, S.A., Boltaev, G.S., Iqbal, M., Kim, V., Ganeev, R.A. and Alnaser, A.S. (2021). Ultrafast fiber laser-induced fabrication of

superhydrophobic and self-cleaning metal surfaces. *Applied Surface Science*, 542, p.148560.

Latthe, S.S., Sutar, R.S., Bhosale, A.K., Nagappan, S., Ha, C.S., Sadasivuni, K.K., Liu, S. and Xing, R. (2019). Recent developments in air-trapped superhydrophobic and liquid-infused slippery surfaces for anti-icing application. *Progress in Organic Coatings*, 137, p.105373.

Lee, C., Choi, C.H., and Kim, C.J. (2008). Structured Surfaces for a Giant Liquid Slip. *American Physical Society*, 101(6).

Lee, C., and Kim, C.J. (2009). Maximizing the Giant Liquid Slip on Superhydrophobic Microstructures by Nano Structuring Their Sidewalls. *Langmuir*, 25(21), pp.12812–12818.

Ma, Q., Tong, Z., Wang, W. and Dong, G. (2018). Fabricating robust and repairable superhydrophobic surface on carbon steel by nanosecond laser texturing for corrosion protection. Applied Surface Science, 455, pp.748–757.

Merlin, P.W. (2020) *Green Light for Green Flight*: Washington, DC: NASA.

Ngo, C.C., and Gramoll, K. (2010). Multimedia Engineering Fluid Mechanics. [online] eCourses. Available at: https://ecourses.ou.edu/cgi-bin/ebook.cgi?doc=&topic=fl [Accessed 20 Oct. 2022].

Ou, J., Perot, B. and Rothstein, J.P. (2004). Laminar drag reduction in microchannels using ultrahydrophobic surfaces. *Physics of Fluids*, 16(12), pp.4635–4643.

Rasitha, T.P., Vanithakumari, S.C., George, R.P. and Philip, J. (2019). Template-Free One-Step Electrodeposition Method for Fabrication of Robust Superhydrophobic Coating on Ferritic Steel with Self-Cleaning Ability and Superior Corrosion Resistance. Langmuir, 35(39), pp.12665–12679.

Rothstein, J.P. (2010). Slip on Superhydrophobic Surfaces. Annual Review of Fluid Mechanics, 42, pp.89-109.

Sampathkumar, V., Ambar, C., Thinaharan, C., Ram, G., George, R.P., Kaul, R., Kushvinder, B., John, P. (2021). Laser patterned titanium surfaces with superior antibiofouling, superhydrophobicity, self-cleaning and durability: Role of line spacing. Surface and Coatings Technology, 418, p.127257.

Shop3D.ca (2020). 3D Printing Metal Parts: Methods and Cost. [online] Available at: Shop3D.ca.

Tam, J., Palumbo, G. and Erb, U., 2016. Recent Advances in Superhydrophobic Electrodeposits. *Materials*, 9(3), p.151.

Tanvir, K.M. and Kietzig, A.M. (2016). Drag reduction on laser-patterned hierarchical superhydrophobic surfaces. Soft Matter, 12(22), pp.4912–4922.

Thurston, S. and Jones, R.D. (1965). Experimental model studies of non-Newtonian soluble coatings for drag reduction. *Journal of Aircraft*, 2(2), pp.122–126.

Wenzel, R.N. (1936). Resistance of solid surfaces to wetting by water. *Industrial & Engineering Chemistry*, 28(8), pp.988–994.

Xu, L., Liu, F., Liu, M., Wang, Z., Qian, Z., Ke, W., Han, E.H., Jie, G., Wang, J. and Zhu, L. (2019). Fabrication of repairable superhydrophobic surface and improved anticorrosion performance based on zinc-rich coating. Progress in Organic Coatings, [online] 137, p.105335.

Young, T. (1805). III. An essay on the cohesion of fluids. *Philosophical Transactions of the Royal Society of London*, 95, pp.65–87.

Zhang, D., Wang, L., Qian, H. and Li, X. (2015). Superhydrophobic surfaces for corrosion protection: a review of recent progresses and future directions. *Journal of Coatings Technology and Research*, 13(1), pp.11–29.

ABBREVIATIONS AND SPECIFIC SYMBOLS

α – Angle of Attack

b – Slip Length

C_D – Coefficient of Drag

$C_{D,f}$ – Coefficient of Drag due to skin friction

C_L – Coefficient of Lift

CFD – Computational Fluid Dynamics

ERA – Environmentally Responsible Aviation

LE – Leading Edge

NASA – National Aeronautics & Space Administration

NOx – Nitrous Oxides

OpenFOAM – Open-Source Field Operation and Manipulation

PISO – Pressure-Implicit with Splitting of Operators

SFE – Surface Free Energy

Re – Reynolds Number

ROI – Return on Investment

TE – Trailing Edge

ACKNOWLEDGMENT

The Author would like to extend his sincere gratitude to the Aeronautical Engineering Department of General Sir John Kotelawala Defence University, Ratmalana and his supervisors for their expertise, guidance, supervision, and support for the research.

AUTHOR BIOGRAPHIES

Vishal Christopher Perera is a final year undergraduate at the Department of Aeronautical Engineering at the Faculty of Engineering of General Sir John Kotelawala Defence University, Sri Lanka.

SLMD Rangajeewa is a Senior Lecturer at the Department of Aeronautical Engineering at the Faculty of Engineering of General Sir John Kotelawala Defence University, Sri Lanka.